

# **WIND-TUNNEL SIMULATION OF ENVELOPE CONCENTRATIONS FROM RADON EXHAUST VENTILATORS AROUND TYPICAL DOMESTIC BUILDINGS**

**D.E. Neff<sup>1</sup>, R.N. Meroney<sup>2</sup> and H. Elbadry<sup>3</sup>**

1. Research Scientists, Colorado State University, Fort Collins, CO 80523
2. Professor of Civil Engineering, Colorado State University, Fort Collins, CO 80523
3. Assistant Professor, Ain Shams University, Cairo, Egypt.

## **Abstract**

Dispersion of simulated radon releases from short exhaust ventilators on 1:35 scale models of several suburban homes were examined in a boundary-layer wind tunnel to determine the relative dilution which occurs for alternative release configurations. Concentration data were compared to values produced by analytic prediction formulae proposed by Schulman and Scire (1993) and Huber and Snyder (1982) for the downwind recirculation cavity and the far wake, respectively. Gabled roof configurations promoted additional dilution such that measured cavity values fell one to two-orders of magnitude beneath predictions. The near wake concentrations and predicted values were found to be very similar.

## **1.0 INTRODUCTION**

Currently, the U.S. Environmental Protection Agency requires that mitigation exhaust for radon removal be discharged above the eave of a building between eave and roof peak to ensure that very little of the exhaust is re-entrained into the building, and to ensure that exposures are small to persons in the yard or neighboring buildings. This requirement often increases the cost, detracts aesthetically from the home, and can discourage some owners from installing a mitigation system. The objective of this study was to identify whether there are conditions under which the mitigation radon exhaust for typical homes can safely be released at eave edge or grade level. Heating and ventilating designers frequently face similar problems related to releases from chemical fume hoods, short stacks, and air-conditioning units.

Scale models of four different typical suburban homes were constructed at 1:35 scale and tested in a wind tunnel facility. These tests, both visual and concentration measurements, covered four wind directions, three effluent to approach flow wind speed ratios, three release locations and 45 concentration sampling points distributed over the building envelope and downwind. Measured concentrations were also compared against analytic and numerical building downwash calculations in the recirculation cavity and in the far-wake region.

## **2.0 FLUID MODEL DESIGN**

A boundary layer wind tunnel fluid model was designed to assist in the interpretation of relative mitigation of radon exhausts from typical homes. The 1:35 reduced scale models represented:

- 1) Four different generic suburban style homes; a one story home with roof slopes of 6:12 and 9:12 (eave height of 3.51 m, gable heights of 6.55 and 8.08 m, respectively) and a two story home with roof slopes of 6:12 and 9:12 (eave height of 6.10 m, gable heights of 8.08 and 9.07 m, respectively) (see Figure 1),
- 2) A suburban neighborhood with effective equivalent surface roughness,  $Z_0$ , equal to 0.3 m, resulting in an approach flow boundary layer providing equivalent surface velocity and turbulence profiles, and
- 3) Vent gas stack geometries and discharge typical of radon exhaust designs, ie. stack diameter of 10.2 cm and exhaust flow rates from  $10 \times 10^3$  to  $50 \times 10^3$  ccs..

All model tests were performed in the Environmental Wind Tunnel (EWT) test facility at Colorado State University (CSU). This tunnel has a 3.66 m by 2.13 m cross-section, a 17.4 m length, a wind speed range of 0 to 13 m/s and a flexible test section roof. The suburban home models were placed 13.6 meters from the start of the EWT's test section. The development of suburban boundary-layer winds at a reduced scale of 1:35 with an equivalent surface roughness of 0.3 m or a power-law exponent of 0.2 required the placement of a turbulence generating grid at the upwind edge of the model turntable. Figure 2 shows an elevation view of the wind tunnel turntable layout used for this project (note all units are model scale centimeters).

The buildings were oriented for four approach wind directions,  $0^\circ$ ,  $45^\circ$ ,  $90^\circ$  and  $180^\circ$ . Given the symmetries of the exhaust locations and building shape these primary wind directions reproduced conditions for the probable distribution of maximum concentrations. Three exhaust locations were studied: a 0.46 m tall mid-roof location, a 0.3 m tall at-eave location and a 0.76 m above-grade wall location. Since all tests were for a neutrally buoyant plume in a neutral atmospheric stability each model test condition can be scaled to any field condition where velocity ratio equality (exhaust to approach flow,  $W/U$  is maintained. To cover a wide range of exhaust velocities and approach flow wind speeds three  $W/U$  velocity ratios were examined, 0.25, 1.0, and 2.5. Model wind speed at an equivalent field height of 10 m was set to 400 cm/s. Thus, the model Reynolds number based on building height and wind speed was greater than 22,000 and 38,000 for the one and two-story houses, respectively. The resulting minimum surface roughness Reynolds number,  $Re_* = uZ_0/\nu$ , was 1905, and the stack Reynolds number,  $Re_s$ , ranged from 161 to 1613.

### 3.0 FLUID MODEL TEST PROGRAM

#### 3.1 Instrumentation

Single-hot-film anemometer probes and pitot-static pressure probes were used to measure velocity statistics. Velocities and turbulence were measured with a precision of  $\pm 10\%$ , completeness of 99% and representativeness of  $\pm 5\%$ .

Concentrations were measured using a flame ionization type gas chromatograph, a 50 unit gas-sampling system, and a 100% ethane source simulant. Forty five sampling locations were distributed over the surface of the model building and in the wake of the building for 144 different run conditions. The sampling locations located on the building surface are shown in Figure 3. The sampling locations located downwind of the building are shown in Figure 4. Normalized concentrations are believed to be accurate to  $\pm 5\%$  or 1.5 ppm whichever is greater. The data has a completeness of 98% and a representativeness of  $\pm 17\%$ .



### 3.2 Wind Field Verification Tests

The approach flow velocity and turbulence were arranged to be similar to atmospheric flow over a suburban type roughness condition. Lateral and longitudinal profiles were measured to assess flow homogeneity. Lateral variations were minor, and wind and turbulence profiles were judged satisfactory, Figure 5. Wind profiles and concentration measurements were also made at three different wind speeds (300, 400 and 500 cm/s) to assess Reynolds number independence of the test data. Dimensionless wind speed and turbulence profiles were essentially equivalent at all speeds tested, and dimensionless concentrations,  $K = \chi u/Q$  [ $m^{-2}$ ], varied with mean wind speed and replication no more than 5 to 20 % at building surface and plume centerline locations.

To verify the equivalent atmospheric dispersion condition a passive ground level source was placed 50 cm upwind of the model center position. The model house was removed, and a concentration sampling grid was placed downwind. Surface, cross-wind and vertical concentration profiles were compared against classical Pasquill-Gifford Gaussian plume model predictions. The passive model plume was found to replicate C-D Pasquill-Gifford dispersion conditions over the test region..

### 3.3 Exhaust Release Tests

Flow visualization of the effluent plume motion for 96 different conditions was documented on video cassette VHS tape. The camera was positioned 45° away from looking upwind and focused primarily on the plume behavior in the vicinity of the exhaust stack and building only. The flow visualization documented the plume trajectories from the model stacks and cases of downwash and plume entrainment into the building recirculation cavity. Experiments revealed that exhaust vents located downwind of the roof peak operated at low exhaust velocities released plumes which recirculated significantly in the building cavity region.

Concentration measurements were obtained at 45 sample locations for 144 different run conditions: four building shapes, four wind orientations, three stack locations, and three exhaust velocity ratios. Resultant concentration data are presented in the form of concentration coefficients  $K = CU/Q$  [ $m^{-2}$ ] as bar charts to facilitate comparisons.

## 4.0 AIR-POLLUTION AERODYNAMIC MODELS

The concentration field produced by a source located near the ground in the vicinity of buildings can be significantly modified from that predicted by conventional diffusion formulae. Such formulae contain the implicit assumptions that the flow field has straight parallel streamlines, modest velocity gradients, and distributions of turbulence energy and length scales which result from surface features that remain unchanged over long distances. Near buildings the flow field becomes highly complex. Curved streamlines, sharp velocity discontinuities, and non-homogeneous turbulence disperse effluent in a complicated manner related to source configuration and building geometry.

In the immediate lee of the building, there is a cavity region where recirculation occurs, mean velocities are reduced and the air flow is highly turbulent. The flow in the building wake farther downstream is characterized by a high turbulence intensity and mean velocity deficit that eventually decays to background levels. The complex flow patterns induced by the building prohibit reliable determination of air quality concentrations close to buildings through the use of the basic Gaussian plume model and associated dispersion parameters without substantial modification. General reviews of experimental data and mathematical models have been prepared by Meroney (1982) and Hosker (1984).

Different models were suggested for calculating the concentration in the near-wake (the recirculation cavity) and in the far-wake downstream of the building. In this report the Schulman and Scire model (1993) was used to predict the concentration in the near-wake, and the Huber and Snyder model (1982) was used to calculate the far-wake concentrations.

#### 4.1 Dispersion in the Recirculation Region

Schulman and Scire (1991) suggested a model that estimates the concentrations at the building roof, downwind wall and near wake recirculation cavity for winds perpendicular to the building sides. They proposed another model (Schulman and Scire, 1993) for estimating concentrations solely in the recirculation cavity. The first model (Schulman and Scire, 1991) computed a total concentration by considering separately the contribution of the portions of the plume below and above the high turbulence region.

$$\chi = f_1 C_1 + f_2 C_2$$

where  $f_1$  and  $f_2$  are the fractions of the plume below and above the high turbulence region,

$$C_1 = \frac{B_o Q}{U s^2}$$

and

$$C_2 = \frac{B_o Q}{U s^2} e^{-(Hs-H+\Delta h)^2/2\sigma_z^2} \quad \text{for roof receptors}$$

$$C_2 = \frac{B_o Q}{U s^2} e^{-(Hs+\Delta h)^2/2\sigma_z^2} \quad \text{for ground-level receptors}$$

where  $B_o$  is an empirical constant approximately equal to 16 (ASHRAE, 1989),  $s$  is the stretched string distance between stack base and receptor, and the vertical dispersion coefficient  $\sigma_z$  is

$$\sigma_z = 0.21 R^{0.25} x^{0.75}$$

Schulman and Scire (1993) suggested another model which computes the ground-level concentration in the down-wind recirculation cavity by considering the fraction of the plume below the cavity height  $H_R$ .

$$\chi = f_c C_c$$

with

$$C_c = \frac{B_o Q}{B_o w_o A_o + U s^2}$$



where  $f_c$  is the portion of the plume below  $H_R$  at the end of the cavity,  $w_o$  is the exhaust speed from the stack and  $A_o$  is the stack or exit face area.

#### 4.2 Dispersion in the Building Wake Region

Gaussian plume models are routinely applied in studies of environmental impact. The Gaussian plume equation for estimating normalized concentration is

$$\frac{\chi U}{Q} = \frac{1}{2\pi\sigma_y\sigma_z} e^{-y^2/2\sigma_y^2} [e^{-(z-h)^2/2\sigma_z^2} + e^{-(z+h)^2/2\sigma_z^2}]$$

where  $\chi$  = pollutant concentration ( $\text{g m}^{-3}$ ),  
 $U$  = mean wind speed affecting the plume ( $\text{m s}^{-1}$ ),  
 $Q$  = emission rate ( $\text{g s}^{-1}$ ),  
 $h$  = effective emission height above the ground (m), and  
 $\sigma_y, \sigma_z$  = the values of the horizontal and vertical dispersion.

This form assumes that the plume spread has a Gaussian distribution, the wind affecting the plume is uniform, and the plume is perfectly reflected at the surface.

A variety of modifications to the basic Gaussian plume model have been suggested by different researchers to provide estimates of concentrations in the far wake of buildings. These modifications are based on estimating enhanced dispersion parameters. Huber and Snyder (1982) suggested a model which is based on the concept that the scale of mixing is related to the length scales of the building. The modified  $\sigma_z'$  equation for a building where  $W_b \geq H_b$  is given by:

$$\sigma_z' = 0.7H_b + 0.067(x-3H_b) \quad \text{for } 3H_b \leq x < 10H_b$$

or

$$= \sigma_z \{x + x_z\} \quad \text{for } x \geq 10H_b$$

where  $x_z$  is a virtual source distance such that  $\sigma_z(0.01H_b) = 1.2 H_b$ .

For a building  $W_b < H_b$  Huber and Snyder suggest that the modified  $\sigma_z'$  equation is given by:

$$\sigma_z' = 0.7W_b + 0.067(x-3W_b) \quad \text{for } 3W_b \leq x < 10W_b$$

or

$$= \sigma_z \{x + x_z\} \quad \text{for } x \geq 10W_b$$

Note that  $\sigma_z'$  is not permitted to be less than the point source value.

For  $W_b \geq H_b$  and a building width to building height ratio  $W_b/H_b$  less than or equal to 5, the modified  $\sigma_y'$  equation is given by:

$$\sigma_y' = 0.35W_b + 0.067(x-3H_b) \quad \text{for } 3H_b \leq x < 10H_b$$

or

$$= \sigma_y \{x + x_y\} \quad \text{for } x \geq 10H_b$$

where  $x_y$  is a virtual source distance such that  $\sigma_y(0.01W_b) = 1.2 W_b$ .

For  $W_b \geq H_b$  and building width to building height ratios  $W_b/H_b$  greater than 5, the available data are insufficient to provide general equations for  $\sigma_y$ . For a building that is much wider than it is tall and a stack located toward the center of the building (i.e., away from either end), only the height scale is considered to be significant. The modified  $\sigma_y$  equation is then given by:

$$\sigma_y' = 0.35H_b + 0.067(x-3H_b) \quad \text{for } 3H_b \leq x < 10H_b$$

or

$$= \sigma_y\{x + x_y\} \quad \text{for } x \geq 10H_b$$

For  $W_b \geq H_b$ ,  $W_b/H_b$  greater than 5 and a stack located laterally within about  $2.5 H_b$  of the end of the building, lateral plume spread is affected by the flow around the end of the building. With end effects, the enhancement in the initial lateral spread is assumed to be given by:

$$\sigma_y' = 1.75H_b + 0.067(x-3H_b) \quad \text{for } 3H_b \leq x < 10H_b$$

or

$$= \sigma_y\{x + x_y\} \quad \text{for } x \geq 10H_b$$

The modified  $\sigma_y$  equation for ( $W_b < H_b$ ) building is given by:

$$\sigma_y' = 0.35W_b + 0.067(x-3W_b) \quad \text{for } 3W_b \leq x < 10W_b$$

or

$$= \sigma_y\{x + x_y\} \quad \text{for } x \geq 10W_b$$

## 5.0 WIND-TUNNEL CONCENTRATION MEASUREMENTS AND MODEL COMPARISONS

### 5.1 Results from the Wind-tunnel Measurement Program

Figure 6 displays bar charts comparing the influence of building shape on concentration patterns for selected run conditions. Figure 7 displays bar charts comparing the influence of exit velocity ratio on concentration patterns for selected run conditions. Figure 8 displays bar charts comparing the influence of wind direction on concentration patterns for selected run conditions. Note that the values in these tables and figures are  $K_p * 10^4$ .

To determine sample concentration,  $\chi$ , in pCi/L for different source strengths,  $Q_{ss}$ , in pCi/L the following equation was used:  $\chi$  [pCi/L] =  $(K_p[m^{-2}] * (W/U_H) * (Area[m^2]) * (Q_{ss}[pCi/L])$  where "Area" is the cross-sectional area of the exhaust pipe. Whenever the maximum concentration was below the atmospheric background value of 0.4 pCi/L background was assumed. Figure 9 displays a bar chart comparing the release location's influence on maximum observed concentration in pCi/L.

### 5.2 Wind-Tunnel Data Analytic Model Comparisons

For thirty six run combinations the Schulman and Scire (1993) model was used to calculate cavity concentrations downwind of the prototype buildings. The 180° wind direction was not calculated using the model since the concentrations were at back-ground level. The stretched-string distance between the



stack base and the receptor was calculated for each situation. The fact that the stack is located in the wake of the building resulted in using a value of one for the coefficient  $f_c$ . Figure 10 illustrates the release locations' influence on calculated maximum concentrations for source strength equal to 1000 pCi/L. The model results are generally conservative estimates of the observed values in the experiments (see Figures 9 and 10). The model over predicts the concentrations, and the predicted concentrations are often one to two order of magnitude higher than the observed concentration especially in areas closer to the stack. The model applies for rectangular buildings where the wind is perpendicular to the building sides. Applying the model for sloped roof buildings where the stack is in the recirculation cavity is probably not appropriate, and a new model should be developed for such conditions.

The Huber and Snyder model (1982) was used to predict the concentrations for  $x \geq 3 H_b$  downwind of the building for all the experiment combinations. Figure 10 displays the bar charts comparing the release locations' influence on maximum calculated concentrations for source strength equal to 1000 pCi/L. The model predicts concentrations of the same order of magnitude as the wind tunnel results found in Figure 9.

## 6.0 CONCLUSIONS

- 1) Exhaust gases will recirculate heavily in the house wake for all three effluent sources tested whenever the stacks are located downwind of the roof crest,
- 2) The at-grade wall release location usually leads to the highest building surface concentration values. The eave release location leads to somewhat higher concentrations than the roof release location, and
- 3) Source strengths of 100 pCi/L produced concentrations greater than the design value of 1 pCi/L only for wall releases, and even the maximum of these was only 1.4 pCi/L. Source strengths of 1000 pCi/L produced concentrations greater than a design value of 1 pCi/L at sampling locations for all three effluent release locations.
- 4) The Schulman and Scire (1993) model predictions in the building recirculation region are generally conservative. The model over predicts often by one-to two orders of magnitude.
- 5) The Huber and Snyder (1982) far wake model ( $> 3$  building heights downwind) predicted concentrations of the same order of magnitude as the wind tunnel results.

## ACKNOWLEDGEMENTS

The authors wish to express their appreciation for support from Dr. Bruce Henschel, Air and Energy Engineering Research Laboratory, Environmental Protection Agency, Research Triangle Park, NC

## REFERENCES

- ASHRAE (1989), " Air flow around buildings," Chapter 14 in *ASHRAE Handbook-Fundamentals*, Atlanta, American Society of Heating, Refrigerating, and Air-Conditioning Engineers, Inc.
- Hanna S. R., Briggs G. A. and Hosker R. P. (1982), *Handbook on atmospheric diffusion*, Technical Information Center U. S. Department of Energy.
- Hosker, R. P., Jr. (1984), "Flow and Diffusion Near Obstacles," *Atmospheric Science and Power Production*, DOE/TIC-27601, pp. 241-326.
- Meroney, R. N. (1982), "Turbulent Diffusion Near Buildings," Chapter 11 in book, *Engineering*

- Meteorology*, E. J. Plate, editor, Elsevier Scientific Pub. Co., Amsterdam, pp. 481-525,
- Meroney, R.N (1990), Bluff-Body Aerodynamics Influence on Transport and Diffusion," *Journal of Wind Engineering and Industrial Aerodynamics*, Vol. 33, pp. 21-33.
- Neff, D.E., Elbadry, H., and Meroney, R.N. (1994), "Physical and Numerical Modeling to Evaluate ASD Exhaust Design for Acceptable Re-entrainment and Dispersion in Houses", Research Report, U.S. Environmental Protection Agency, Air and Energy Engineering Research Laboratory, Research Triangle Park, NC
- Schulman, L.L. and Scire, J.S. (1993), "Building downwash screening modeling for the downwind recirculation cavity," *Journal of Air & Waste Management Association*, Vol. 43, pp. 1122-1127.
- Schulman L. L. and Scire J. S. (1991), " The effect of stack height, exhaust speed, and wind direction on concentrations from a roof-top stack," *ASHRAE Trans.*, Vol. 97 (2), pp. 573.

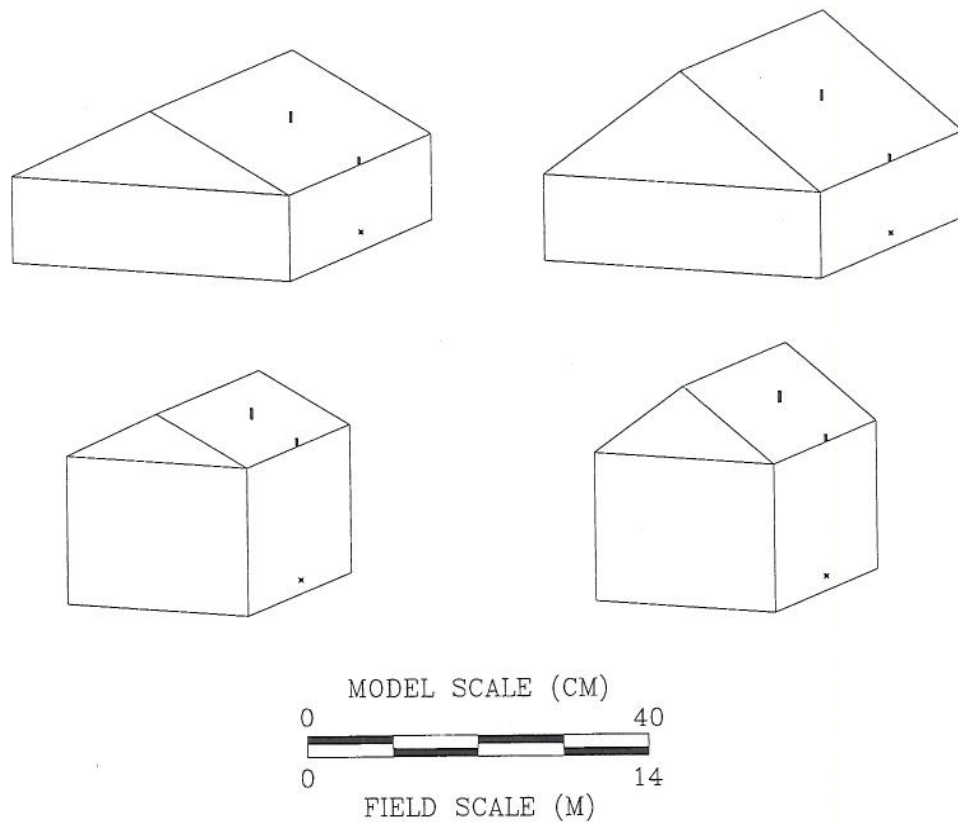


**Figure 1** Schematics of one and two-story houses with 6:12 and 9:12 roof slopes scaled at 1:35.



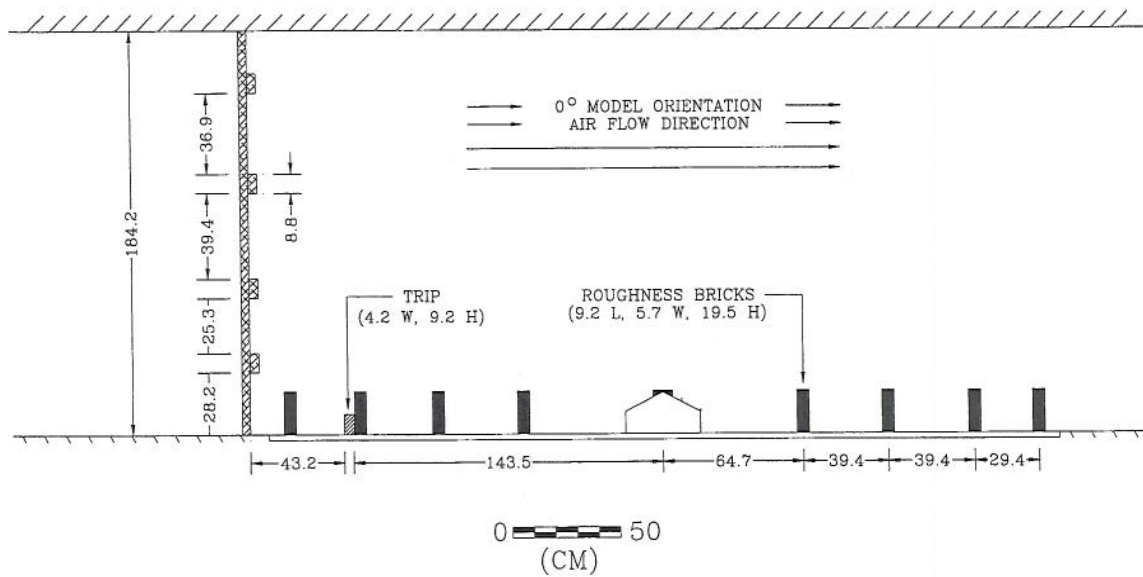
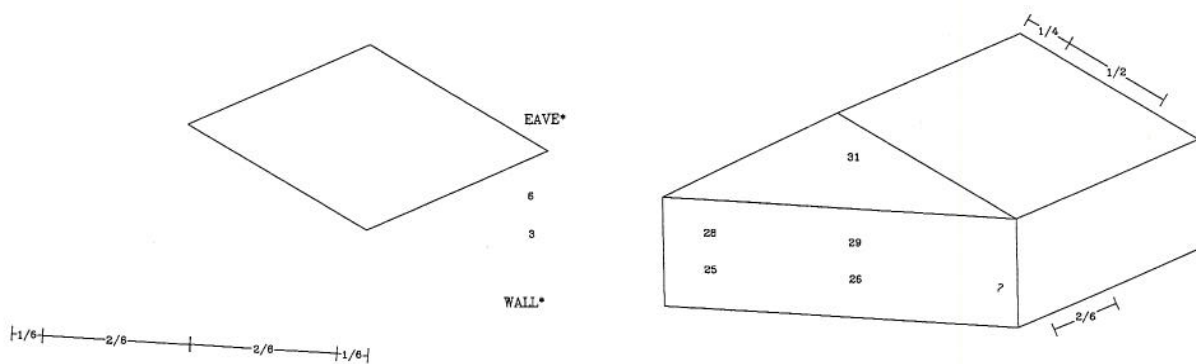


**Figure 2** Wind-tunnel model area elevation view including upstream turbulence grid, trip, roughness elements and model house location.



(DIMENSIONS REPRESENT RELATIVE DISTANCE)

+ : SAMPLE PORT  
 \* : EXHAUST LOCATION

**Figure 3** Sample locations over surface of model domestic houses.

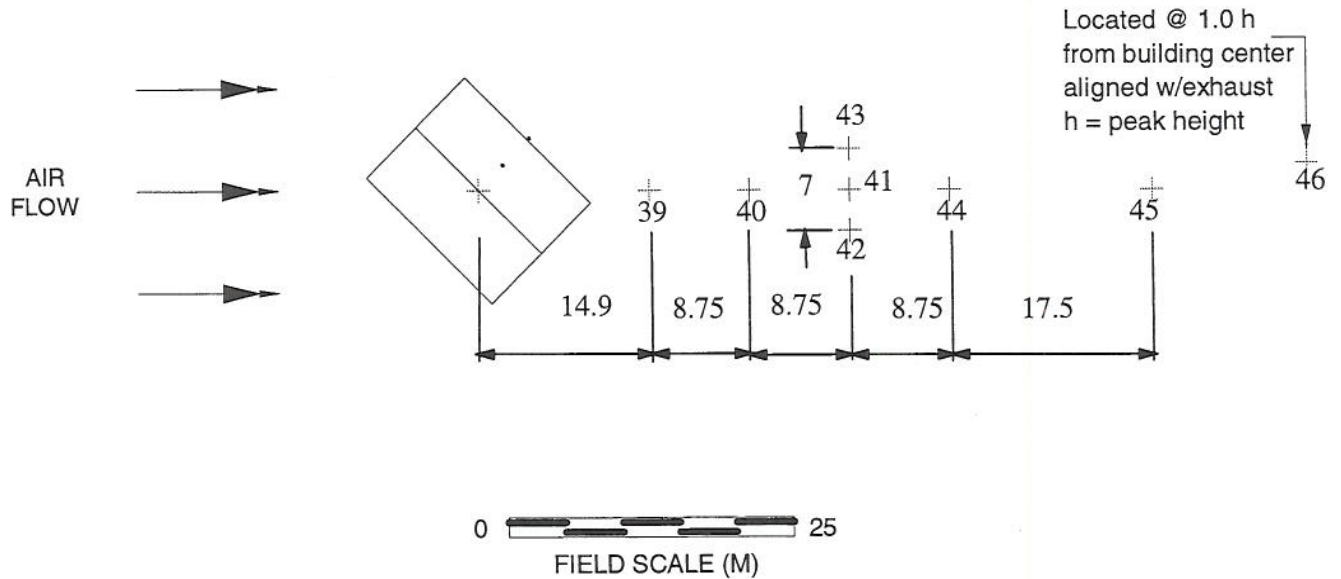


**Figure 4** Sample locations in wake of model domestic house. Typical arrangement show for 45° wind approach angle.

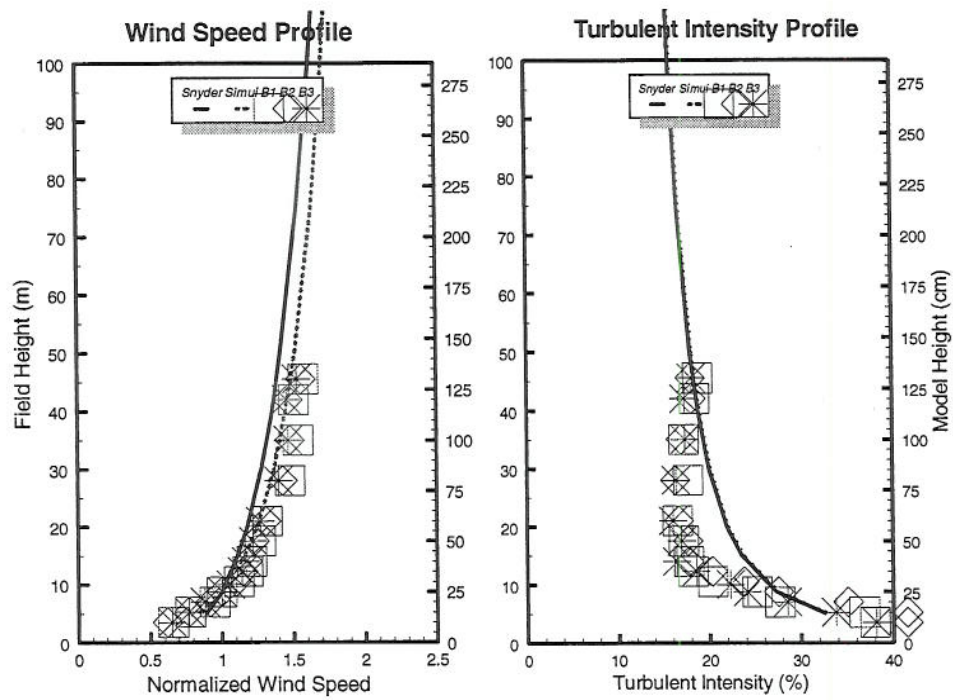


**Figure 5** Wind-tunnel velocity and turbulence profiles measured at model house location for  $U_\delta = 3.0$  (B1), 4.0 (B2) and 5.0 (B3) m/sec.



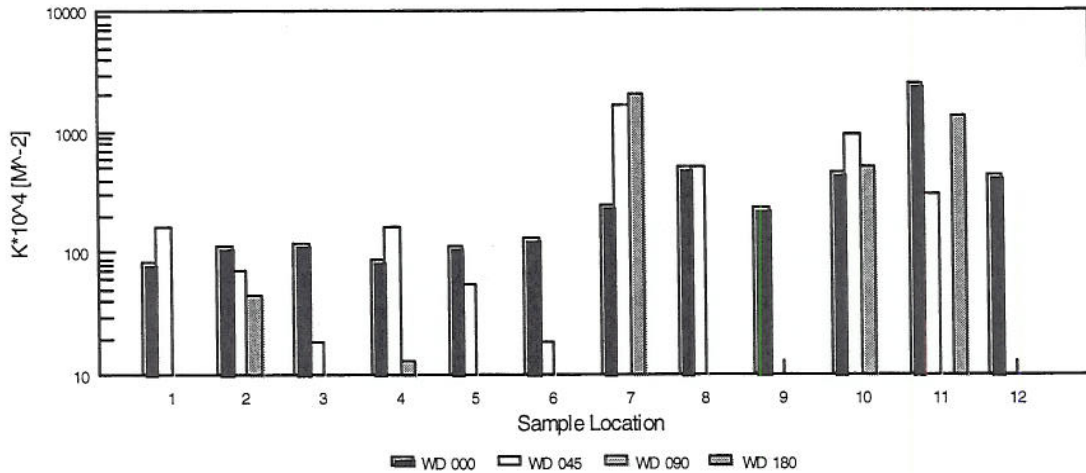


**Figure 6** Wind-tunnel concentration comparisons of the effect of house shape; roof release,  $W/U = 1$ , wind direction =  $0^\circ$ .

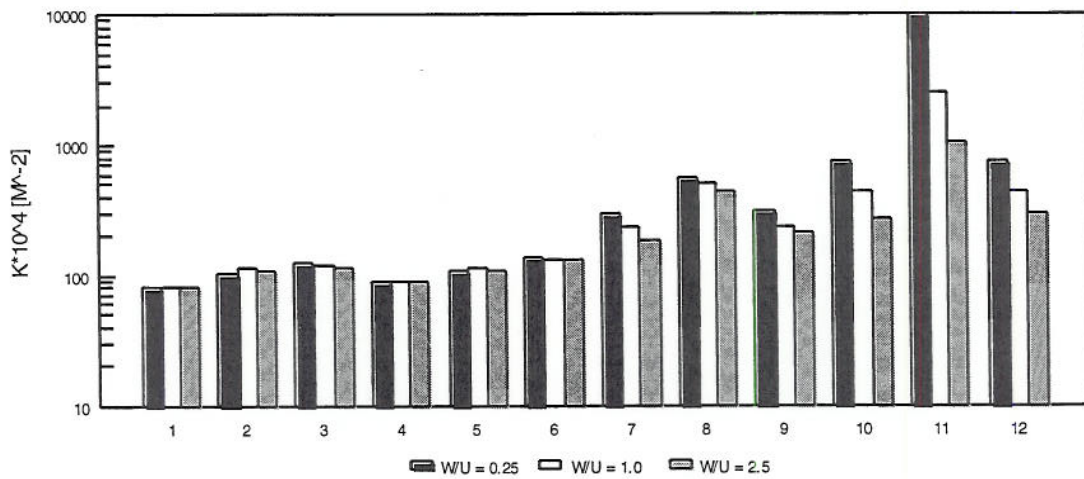


**Figure 7** Wind-tunnel comparisons of the effect of exit velocity ratio; one story house, 6:12 roof slope, wind direction =  $0^\circ$ .

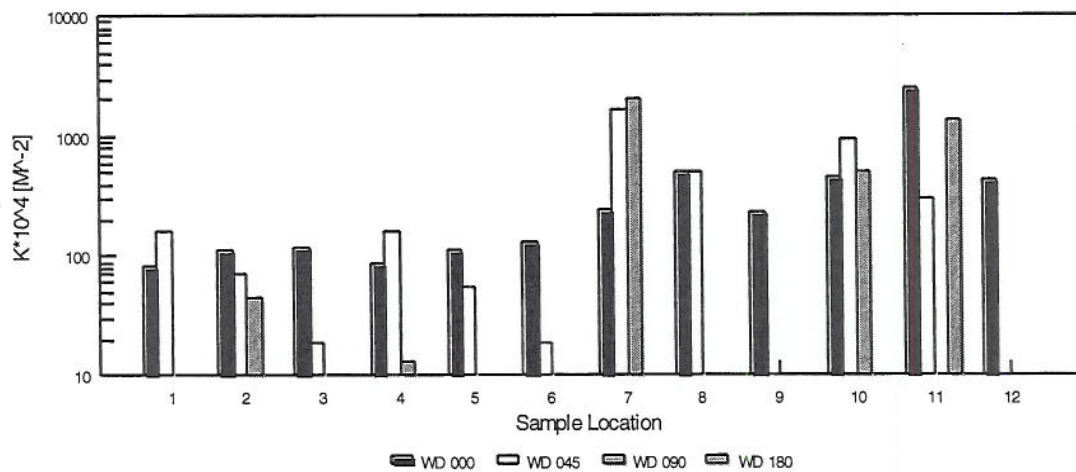


**Figure 8** Wind-tunnel comparisons of the effect of wind direction; One-story house, 6:12 roof slope, roof release,  $W/U = 1.0$ .

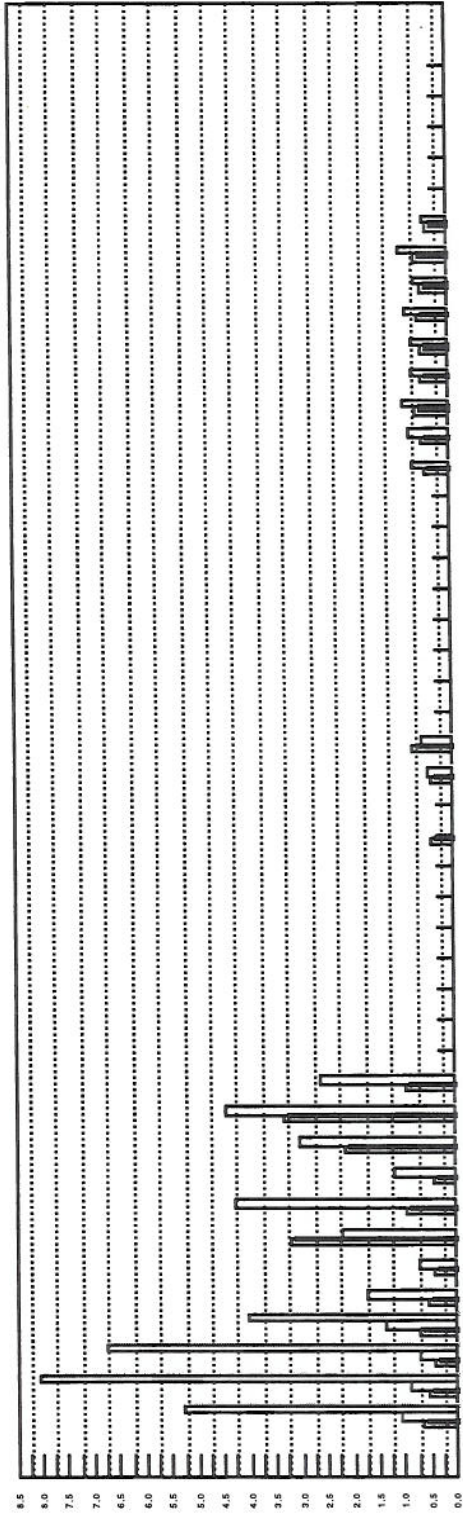


**Figure 9** Maximum measured sample locations over all run conditions for an exhaust source strength of 1,000 cPi/L. Maximum values selected from four building shapes, three exhaust velocity ratios, and four wind directions studied.

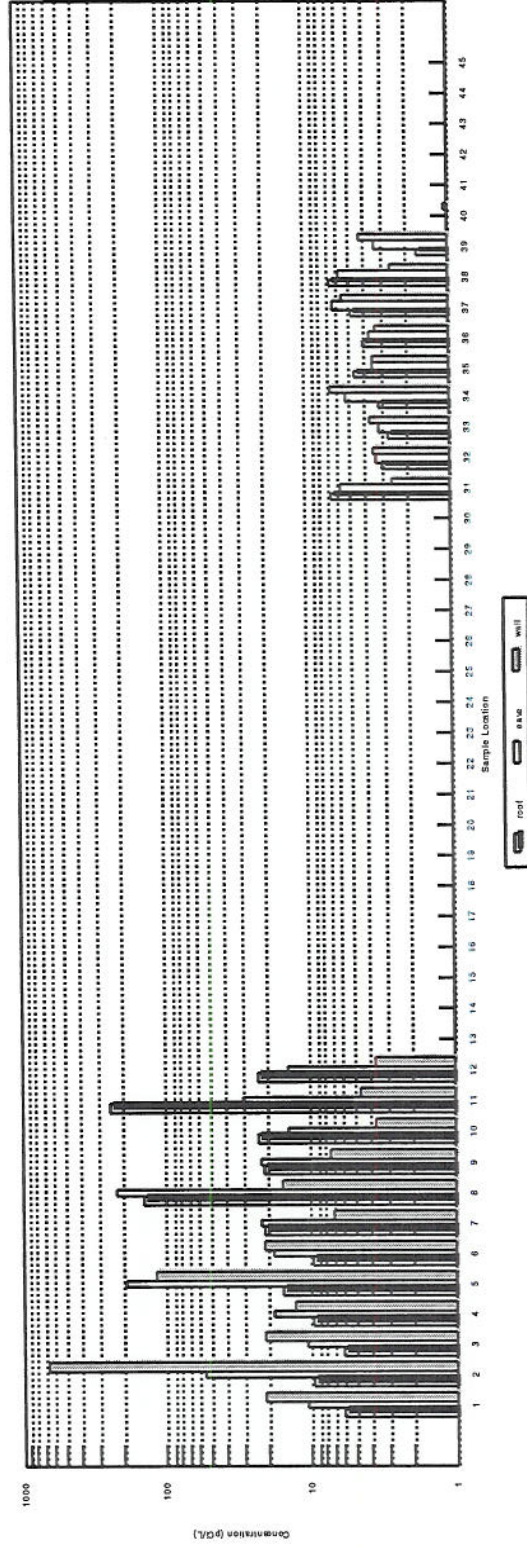


**Figure 10** Maximum sample concentrations calculated over all run conditions for an exhaust flow rate of 1,000 pCi/L. Sample locations 1 through 12 calculated from Schuman and Scire (1993) equations, and sample locations 31 through 45 are calculated from Huber and Snyder (1982) equations.